



Available online at
ScienceDirect
www.sciencedirect.com

Elsevier Masson France
EM|consulte
www.em-consulte.com/en



REVIEW

Magnetic resonance features of pyogenic brain abscesses and differential diagnosis using morphological and functional imaging studies: A pictorial essay

Carmine Franco Muccio^a, Ferdinando Caranci^b,
Felice D'Arco^{b,*}, Alfonso Cerase^c, Luca De Lipsis^d,
Gennaro Esposito^a, Enrico Tedeschi^b, Cosma Andreula^e

^a Unit of Neuroradiology, Department of Neuroscience, Hospital "Gaetano Rummo", Benevento, Italy

^b Unit of Neuroradiology, Department of Advanced Biomedical Sciences, University "Federico II", Naples, Italy

^c Unit of Neuroradiology, Department of Neuroscience, University "Santa Maria alle Scotte", Siena, Italy

^d Department of Critical Care Medicine, Hospital "Fatebenefratelli", Benevento, Italy

^e Unit of Radiology and Neuroradiology, Anthea Hospital, Bari, Italy

Available online 21 June 2014

KEYWORDS

Cerebral abscesses;
Pyogenic abscesses;
Magnetic resonance;
PWI;
DWI;
MR-spectroscopy

Summary The aim of this paper is to illustrate the potential of magnetic resonance imaging (MRI) in diagnosis, differential diagnosis, treatment planning and evaluation of therapy effectiveness of pyogenic brain abscesses, through the use of morphological (or conventional) and functional (or advanced) sequences. Conventional MRI study is useful for the identification of lesions, to determine the location and morphology and allows a correct hypothesis of nature in the most typical cases. However, the differential diagnosis from other brain lesions, such as non-pyogenic abscesses or necrotic tumors (high-grade gliomas and metastases) is often only possible through the use of functional sequences, as the measurement of diffusion with apparent diffusion coefficient (DWI-ADC), proton magnetic resonance spectroscopy (¹H-MRS) and perfusion weighted imaging (PWI), which complement the morphological sequences and provide essential information on structural, metabolic and hemodynamic characteristics allowing greater neuroradiological confidence. Modern diagnostic MRI of pyogenic brain abscesses cannot be separated from knowledge, integration and proper use of the morphological and functional sequences.

© 2014 Elsevier Masson SAS. All rights reserved.

* Corresponding author. Unit of Neuroradiology University "Federico II", via Pansini 5, 80131 Naples, Italy.
E-mail address: darcofel@gmail.com (F. D'Arco).

Introduction

Cerebral abscess is a localized infection of the central nervous system (CNS). It is formed by a central necrotic area surrounded by an external wall (collagen, granulation tissue, macrophages, gliosis).

Abscesses account for 1–2% of brain occupying space lesions in western countries and 8% in developing countries [1]. They are frequent in adults while in only 15–30% of the cases, they involve young patients (< 15 years) [2–5].

Pyogenic brain abscesses are not common, accounting for one third of all the cerebral abscesses [6]. They are caused by cerebral dissemination of bacteria coming from neighbouring infections (sinusitis, otitis, mastotitis) or by hematogenous spread of a remote infection (sepsis); however, in approximately 40% of cases, the primary site of infection remains unknown.

Other causes of cerebral bacterial dissemination in CNS are cranio-facial trauma (with penetration of foreign bodies or bone fragments), meningitis and neurosurgery (iatrogenic infections).

Clinical features are different according to the site of the abscess. Diagnosis is challenging and imaging has a primary role in differentiating brain abscesses from other lesions

that can have similar clinical spectrum. MR is the imaging modality of choice for diagnosis and follow-up of brain abscesses.

The aim of this paper is to analyze the role of combined use of morphological and advanced magnetic resonance imaging (MRI) techniques (diffusion weighted imaging—DWI/ADC; perfusion weighted imaging—PWI; spectroscopy—¹H-MRS) in the diagnosis, differential diagnosis, treatment planning and follow-up of pyogenic abscesses. An extensive review of the literature is also provided.

Etiology and pathogenesis

Bacteria responsible for brain abscesses can be both aerobic (most frequently *Staphylococcus*, *Streptococcus* and *Pneumococcus*) and anaerobic [7]. It is also important to highlight that often there are different kinds of bacteria involved in the formation of an abscess.

The most common localization of a pyogenic abscess in the brain is the supratentorial region, in the subcortical white matter, especially, if they come from hematogeneous spread of a distant infection (Figs. 1 and 4) [8,9].

Abscesses secondary to middle ear otitis are typically located in the temporal lobe or in the cerebellum (Fig. 2).

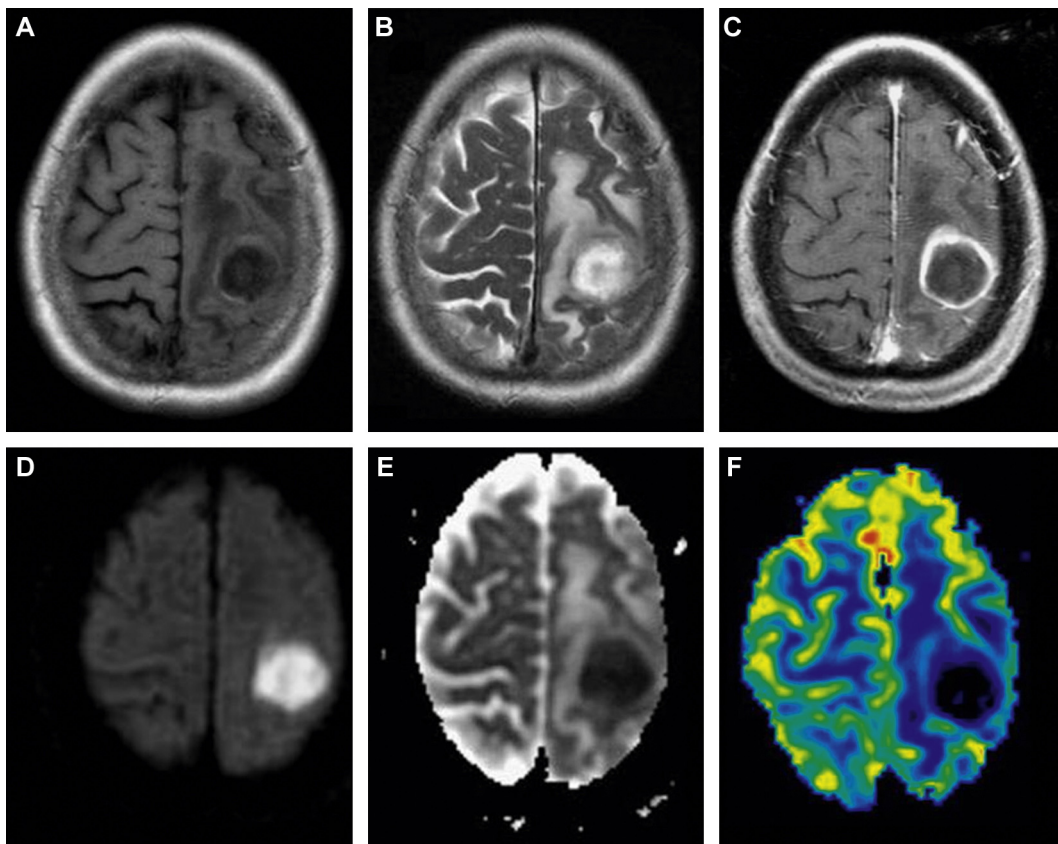


Figure 1 A–F: supratentorial pyogenic abscess in the gray-white junction: T1-weighted (A), T2-weighted (B), gadolinium-enhanced T1-weighted (Gd-MR) (C), DWI ($b = 1000$) (D), ADC (E) and PWI map of CBV (F) MR images. The capsule of the abscess is hyperintense in T1-weighted image (A), partially hypointense in T2-weighted image (B) with surrounding vasogenic oedema. Gd-MR image shows a ring-enhancing mass. The central component of the lesion shows high signal intensity in DWI image (D), and hypointense signal in ADC map, findings that are consistent with restricted diffusion ($ADC = 0.440 \times 10^{-3} \text{ mm}^2/\text{s}$). At PWI, the CBV map (F) does not show evidence of increased perfusion in the gadolinium-enhancing rim ($rCBV = 0.85$).

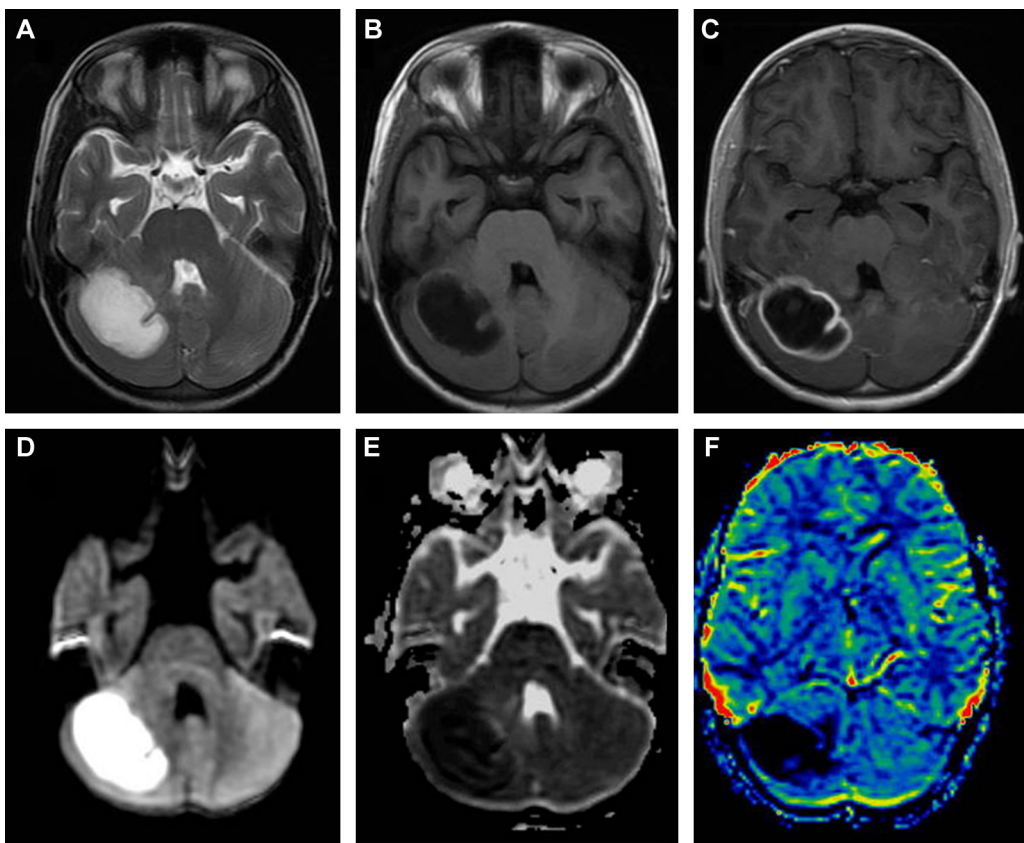


Figure 2 A–F: pyogenic abscess in the right cerebellar hemisphere: T2-weighted (A), T1-weighted (B) gadolinium-enhanced T1-weighted (Gd-MR) (C) magnetic resonance images, DWI ($b=1000$) (D), ADC map (E) and PWI map of CBV (F). The capsule of the abscess is hyperintense in T2-weighted image (A), partially hyperintense in T1-weighted image (B) and shows enhancement in Gd-MR image. The central component of the lesion is hyperintense in T2-weighted image, hypointense in T1-weighted image and shows high signal intensity in DWI image (D) and hypointense signal in ADC map (E), findings that are consistent with restricted diffusion ($ADC = 0.610 \times 10^{-3} \text{ mm}^2/\text{s}$). At PWI, the CBV map (F) does not show evidence of increased perfusion in the gadolinium-enhancing rim of the lesion ($rCBV = 0.9$).

Localization of a pyogenic abscess in the basal ganglia is possible but rare (Fig. 3) [6]. Furthermore, the abscess is often an isolated lesion but, in immunocompromised patients, it is frequent the finding of multiple lesions (Fig. 4).

The early stage of pyogenic infection in the brain is called cerebritis, a localized and blurred area of brain inflammation [10,74]. Cerebritis leads to a cerebral abscess in most of the cases; this evolution consists of four stages:

- early cerebritis (first stage), from the 1st to the 3rd day, characterized by an inflammatory response with predominance of polymorphonuclear leukocytes;
- late cerebritis (second stage), from the 4th to the 9th day, in which the immune response is mediated by lymphocytes and macrophages; central necrosis formation starts with peripheral neoangiogenesis and presence of fibroblasts; the neo-formed vessels have no blood-brain barrier;
- early encapsulation (third stage), from the 10th to the 13th day, in which there is formation of surrounding peripheral wall with central necrosis;
- late capsule stage (forth stage): from the 14th day, characterized by a mature encapsulate brain abscess with a wide central necrotic area.

The presence of air into the abscess is not frequent and is associated with *Clostridium*, *Klebsiella*, *Enterobacter*, *Pectococcus* or *Pseudomonas* [75,76].

Clinical features and treatment

Pyogenic abscesses have non-specific symptoms. In early stages, headache and fever are the most common symptoms but they are not always present. Notably only 30–55% of patients have body temperature above 38.5°C [11]. Focal neurological signs are appreciable in 40–60% of patients depending on the site of the lesion [11]. Complications, not frequent but serious, are intraventricular rupture of the abscess that lead to dissemination of the infection and acute hydrocephalus (Fig. 5), and dural sinus thrombosis.

There are two possible therapeutic choices in case of pyogenic abscess: medical or surgical.

The use of medical therapy alone can be considered in cases of an abscess with < 2.5 cm maximum diameter, localization in not critical areas for the brain function, concomitant meningitis/ependymitis and multiple abscesses [11].

However, the medical treatment alone is often not enough to eradicate the abscess being necessary the

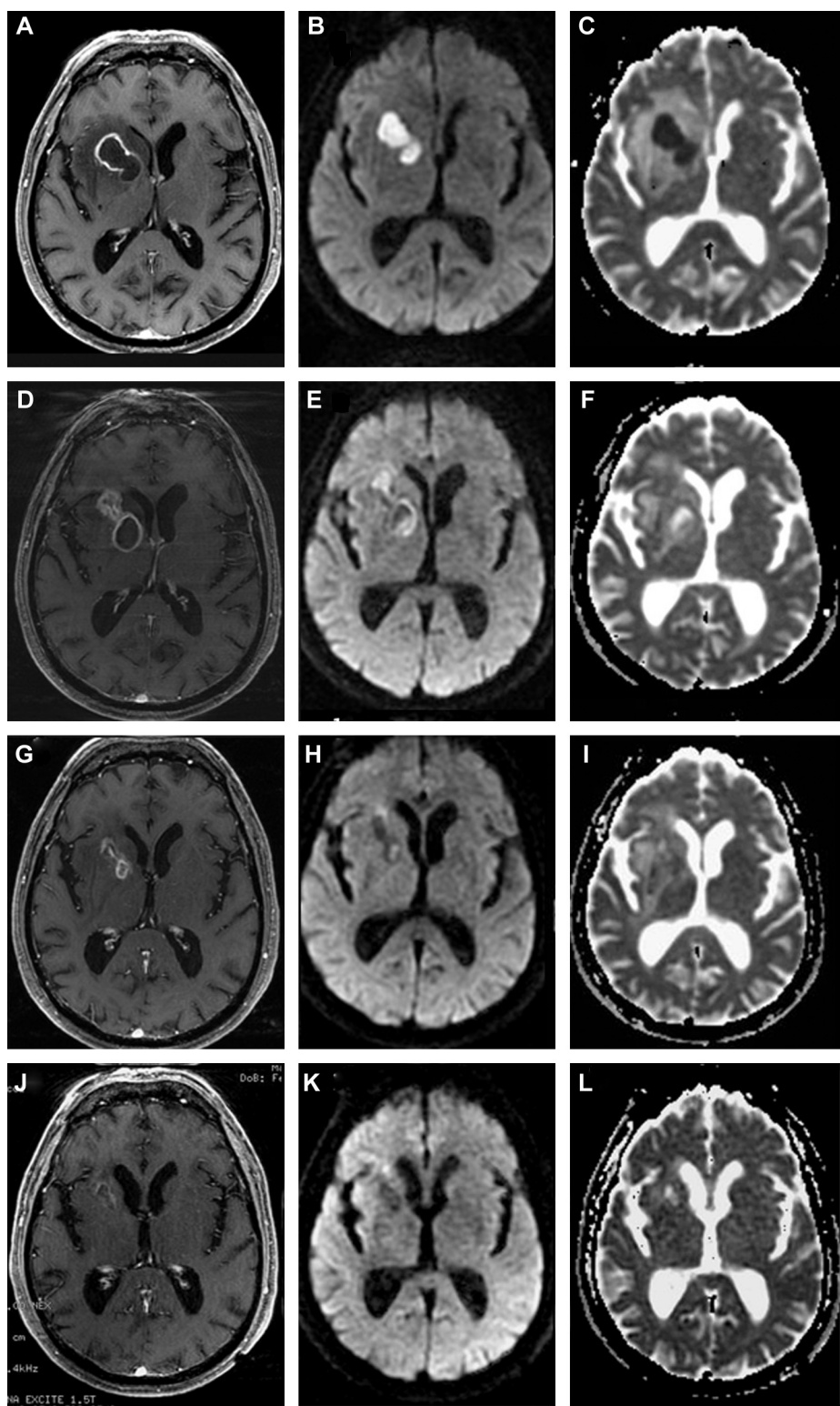


Figure 3 A–N: pyogenic abscess involving the right nucleo-capsular region, and follow-up after stereotactic neurosurgery aspiration and continued antibiotic therapy. At clinical presentation, the abscess shows ring enhancement on gadolinium T1-weighted image (A), high signal intensity on DWI image of the central component (B) and low values on ADC map ($0.434 \times 10^{-3} \text{ mm}^2/\text{s}$) consistent with restricted diffusion (C). Follow-up, after stereotactic aspiration, shows reduction in the size of the abscess cavity on gadolinium-enhanced T1-weighted images (D), dishomogeneous pattern hyper- and hypointense on DWI (E) with increased of ADC values ($1.03 \times 10^{-3} \text{ mm}^2/\text{s}$) (F). One month (G, H, I) and 3 months (L, M, N) follow-up studies, during antibiotic therapy, show further decrease in size of the abscess on T1-weighted images (G, L), low signal intensity on DWI (H, M) and high values on ADC map (I, N), suggesting resolution of the abscess (ADC values at the last follow-up: $1.51 \times 10^{-3} \text{ mm}^2/\text{s}$).

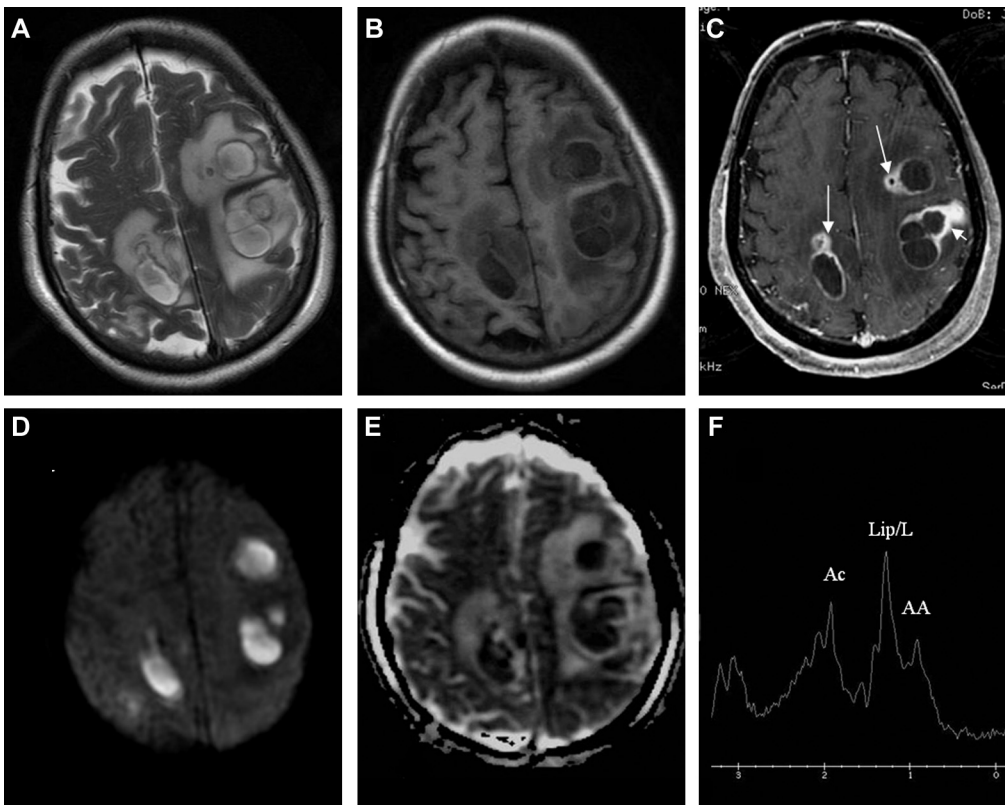


Figure 4 A–F: multiple pyogenic abscesses in immunocompromised patient located at the gray matter junction: T2-weighted (A), T1-weighted (B) and gadolinium-enhanced T1-weighted (Gd-MR) (C) magnetic resonance images, DWI ($b = 1000$) (D), ADC map (E) and ^1H -MRS ($\text{TE} = 144\text{ ms}$). The central component of the abscesses shows dishomogeneous hyperintensity signal in T2-weighted image (A). At Gd-MR image, (C) there are small adjacent satellite lesions by abscesses (arrows) and a thickened capsule on the gray matter (small arrow). The abscesses show hyperintense signal in DWI (D) low signal in ADC map (E), findings that are consistent with restricted diffusion. The ^1H -MRS (F) from the abscess cavity shows resonance representing amino acids (AA), lipids/lactate (Lip/L) and acetate (Ac).

drainage of the necrotic part or the total excision of the mass [73].

Magnetic resonance imaging

MRI shows pyogenic abscess as a round/oval-shaped mass with a central area of suppurative necrosis and a peripheral capsule. The central necrotic area is hypointense to the cerebral white matter on T1-weighted (w) and hyperintense on T2-w images (Fig. 6). However, these features are not always present, being possible, in some cases, a variable T2 signal intensity (Fig. 4).

The external capsule appears typically as a complete hypointense on T2-w and hyperintense on T1-w images rim (Fig. 6) [8,12,13]. The short T1 and T2 of the rim seem to be due respectively to the presence of collagen fibres and to macrophages releasing free radicals with a paramagnetic effect [13]. It is also possible that the external capsule shows a non-typical signal, being hyperintense on T2-w and iso-hypointense on T1-w images (Fig. 2) [8,12,13]. Conversely, the surrounding vasogenic oedema appears hypointense on T1-w and hyperintense on T2-w images (Fig. 6). After intravenous injection of contrast medium (gadolinium), abscess shows a typical peripheral thin and regular "ring enhancement" that corresponds to the T2 hypointense rim (Fig. 6)

[12]. It is important to note that the peripheral contrast enhancement can be stronger in the portion of the abscess closest to the grey matter, because of the stronger inflammatory reaction due to the bigger vascularization of the grey matter [13].

The presence of a satellite abscess (closely associated with a primary abscess) that gives a polylobate appearance to the mass is also possible (Fig. 4) [14].

After surgical and/or medical therapy, the degree of mass effect, surrounding edema, and contrast enhancement decreases slightly but does not change substantially compared with the pre-treatment studies [15].

Advanced MR techniques

DWI-ADC, ^1H -MRS and PWI, together with morphological MRI, can give information about structural, metabolic and hemodynamic features of abscesses helping in differential diagnosis.

Diffusion weighted imaging

DWI gives a critical support in the diagnosis of cerebral abscesses. A pyogenic abscess is typically hyperintense in

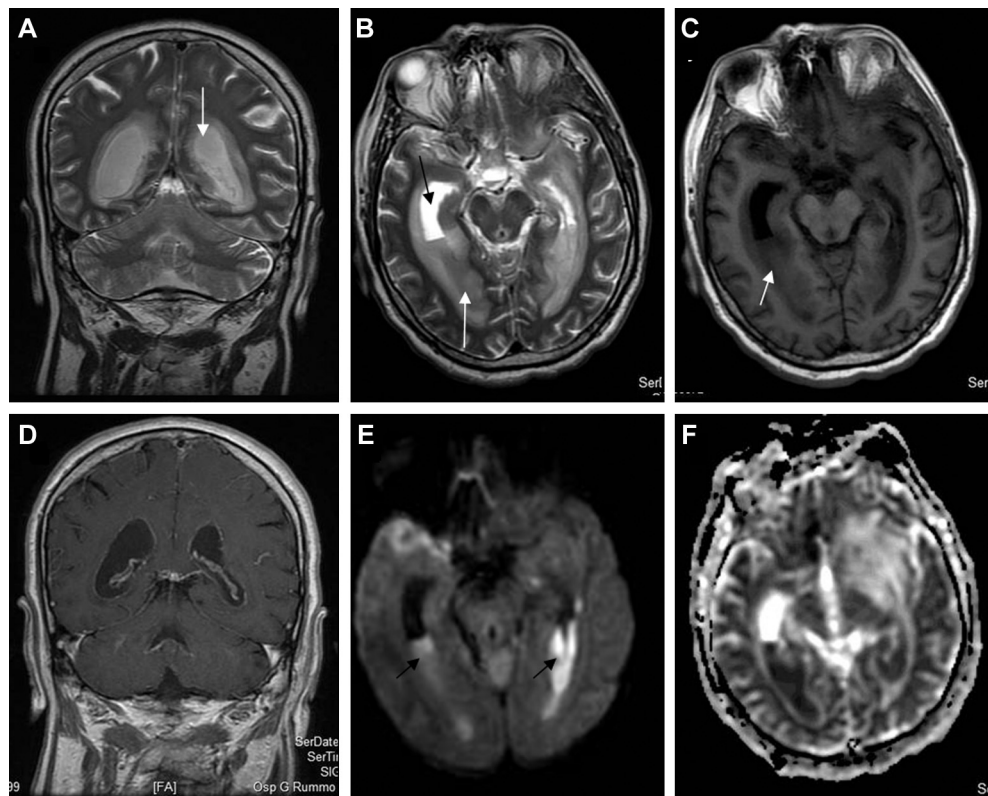


Figure 5 A–F: hydrocephalus following intraventricular rupture of pyogenic abscess: T2-weighted coronal (A) and axial (B), gadolinium-enhanced T1-weighted axial (C) and coronal (D) magnetic resonance images, DWI ($b = 1000$) (E), ADC map (F). In T2-weighted images (A, B), the lateral ventricles are dilatated and the dilute intraventricular pus shows hypointense signal (white arrow) that is less intense in brightness compared with that of the cerebrospinal fluid (CSF) (black arrows). The dilute intraventricular pus is isointense in T1-weighted image (short white arrow) (C), hyperintense in DWI (short black arrows) (E) and low value of ADC ($0.570 \times 10^{-3} \text{ mm}^2/\text{s}$) on the map. Gadolinium-enhanced T1-weighted coronal image (D) shows ependymitis following rupture of abscess.

DWI, with low values on ADC maps (Figs. 1, 2 and 4) because of the water restriction in the central necrotic area containing proteins, bacterial and cellular debris [15–19].

ADC values of the necrotic area in pyogenic abscesses are reported in literature between 0.28 and $0.73 \times 10^{-3} \text{ mm}^2/\text{s}$ [8,20]. However, the different concentration of bacteria and white cells, the different kind of bacteria involved and the immune response of the host can lead to a wider range of

ADC values in the central necrotic area [21]; indeed, there are some cases of pyogenic abscesses with high ADC values in the purulent area [22].

DWI is also useful to improve the diagnosis of an intraventricular rupture of a pyogenic abscess. The purulent fluid appears hyperintense in DWI with low values on the ADC maps in comparison with cerebrospinal fluid (Fig. 7) [23].

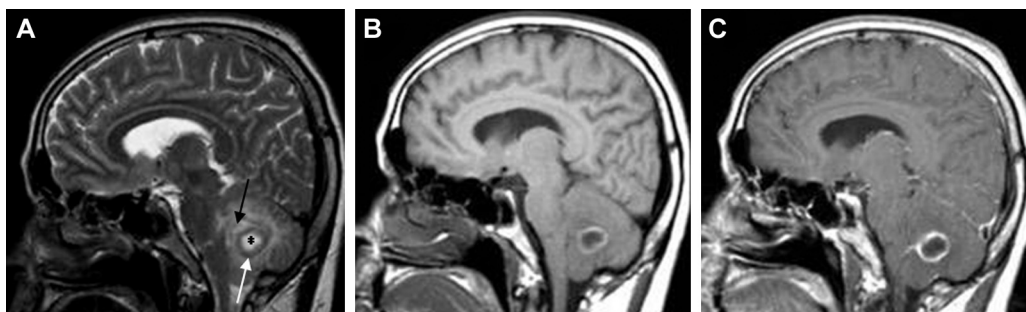


Figure 6 A–C: cerebellar pyogenic abscess: T2-weighted (A), T1-weighted (B) and gadolinium-enhanced T1-weighted MR images. In T2-weighted image, (A) the core of the abscess is hyperintense (asterisk) and the hypointense signal of the capsule (white arrow) is easily distinguishable from peripheral vasogenic edema that appears hyperintense (black arrow). In T1-weighted image after administration e.g. of gadolinium (C) image, the abscess shows an enhanced regular and thin capsule.

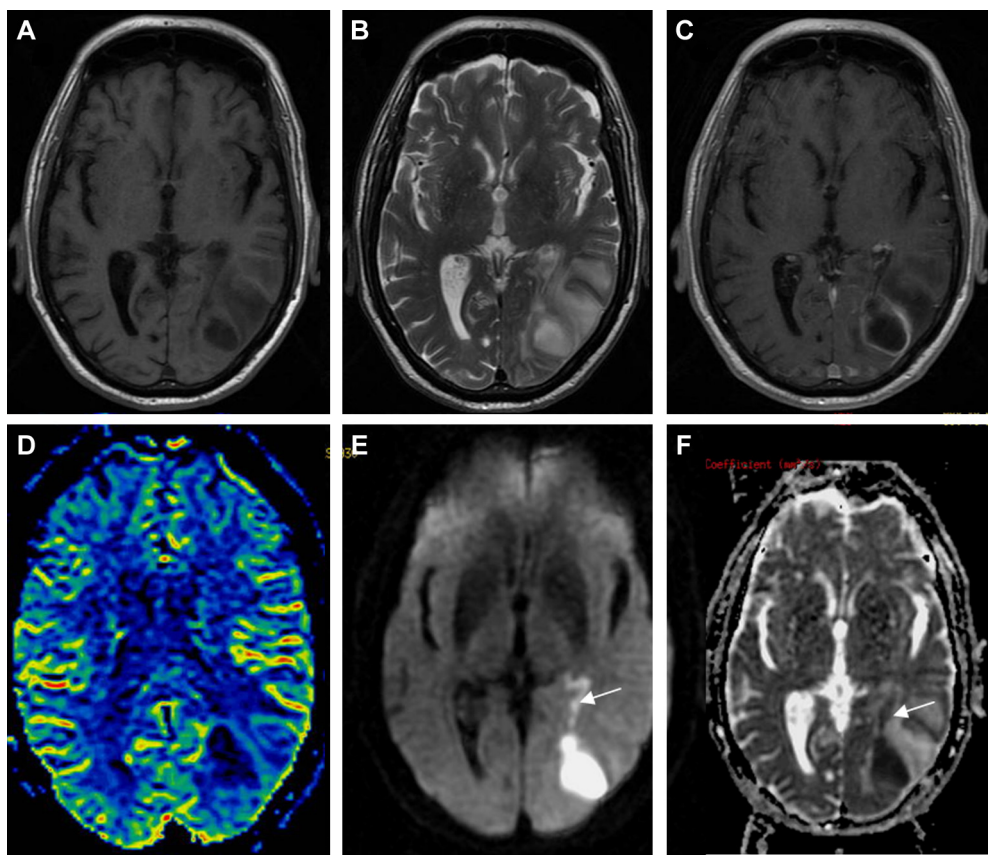


Figure 7 A–F: intraventricular rupture of pyogenic abscess: T1-weighted (A), T2-weighted (B) and gadolinium-enhanced T1-weighted (C) images, PWI map of CBV (D), DWI ($b=1,000$) (E), ADC map (F) MR images. At PWI, the CBV map (D) does not show evidence of increased perfusion in the gadolinium-enhancing rim of the lesion. The central core of the abscess shows high signal intensity in DWI image (E), and hypointense signal in ADC map (F), findings that are consistent with restricted diffusion that extends into trigone of the lateral ventricle (arrow), sign of intraventricular rupture of the abscess.

Some papers suggest the usefulness of DWI in the follow-up of a pyogenic abscess during treatment [15,24,25]. The progressive increase of ADC values could be an earlier index of medical response to antibiotics earlier than the size reduction of the lesion and/or the presence of a gap in the peripheral rim enhancement that are late signs of drug response. Higher ADC values in the central area are also visible after neurosurgical aspiration of the central necrotic area (Fig. 3). On the other hand, constant low ADC values over time would be due to an ineffective therapy, and the recurrence of low ADC values suggests recurrence of active disease.

MR-spectroscopy

MR-spectroscopy ($^1\text{H-MRS}$) is a non-invasive analytical technique that has been used to study metabolic changes in normal and pathological tissues. Typically, the central necrotic area of pyogenic abscesses shows peaks corresponding to lipids (0.8–1.2 ppm), lactate (1.3 ppm) and amino acids (0.9 ppm), without peaks corresponding to normal spectrum of nervous tissue (such as *N*-acetyl-aspartate and choline) [26,27].

Moreover, it is possible to find peaks of alanine (1.5 ppm), acetate (1.9 ppm) and succinate (2.4 ppm) [26,27]. The

absence of choline is related to the lack of normal cell membranes, the absence of *N*-acetyl-aspartate is due to the fact that there are not functioning neurons into the abscess (Fig. 4) [26]. Presence of lactate, acetate and succinate is probably related to bacterial glycolysis and fermentation [27,28]. Amino acids are produced from the proteolysis due to enzymes released by neutrophils [20,28–30] and they are typical in pyogenic abscesses but not always present. In a case series of 194 patients with pyogenic abscesses, Pal et al. found the presence of amino acid peak (alone or associated with other peaks described above) in 80% of patients [31].

$^1\text{H-MRS}$ could be useful in distinguishing between different bacteria responsible for the abscess and in choosing an appropriate therapy [32]. There are three different spectra to consider:

- type A: presence of lactate, amino acids, alanine, acetate, succinate and lipids related to the presence of obligate anaerobes with or without facultative anaerobes;
- type B: presence of lactate, amino acids and occasionally lipids related to obligate aerobes and facultative anaerobes;
- type C: presence of lactate alone, associated with *Streptococcus* and with treated abscesses.

After medical therapy, abscesses show a non-specific peak of lipids and lactate that are also present in cystic tumors [33,34]. For this reason, it is critical to use spectroscopy before the medical treatment [33].

Perfusion weighted imaging

Perfusion weighted imaging (PWI) is an MR technique that gives information about cerebral hemodynamics. Injection of gadolinium leads to a reduction of T2 and T2* signal in the tissue (because of a magnetic susceptibility effect) related to the vascular density [72].

There are few studies about PWI in pyogenic abscesses demonstrating low perfusion (in comparison to the normal white matter) in the abscess capsule (Figs. 1, 2 and 7). Erdogan et al. [35] described four pyogenic abscesses with a mean cerebral blood volume (rCBV) in the capsule of 0.76 ± 0.12 . Muccio et al. [36] described five abscesses with a mean rCBV of 0.72 ± 0.08 . Holmes et al. [37] studied four abscesses with a mean rCBV of 0.79 ± 0.18 . Chan et al. [38] found a mean rCBV of 0.45 ± 0.11 . Finally, Chiang et al., using a 3T scan, found mean values of rCBV of 0.94 ± 0.09 in 20 pyogenic abscesses [51].

In only one paper, Harris et al [39] found rCBV values higher in the abscess capsule than in the normal white matter.

It is possible that perfusion values are related to the stage of the capsule. In early stage, the vascularization is higher than in the late stage in which the fibroblasts are dominant, so explaining the difference in rCBV values between authors [40].

Differential diagnosis

The differential diagnosis between pyogenic abscesses and other brain lesions with a "ring-like" enhancement, such as other kind of abscesses and necrotic tumors, is not always possible with MRI only. The features of the capsule, hypointense on T2-w and hyperintense on T1-w images, with a regular contrast enhancement are often enough to distinguish an abscess from a necrotic tumor that show an irregular central cavity and ill-defined margins with nodules. However, the T2 hypointensity of the capsule and the regular contrast enhancement can be present in non-pyogenic abscesses (*Mycobacterium tuberculosis*, *Toxoplasma*, *Aspergillus*), in some cases of necrotic tumors and in lymphomas [8,12–14,41–45]. The spontaneous peripheral T1 hyperintensity is typical of pyogenic abscesses but can be also present in other lesions, such as mass with peripheral hemorrhagic component or with calcific wall (granulomas, multiple sclerosis plaques, primary brain tumors, metastases, non-pyogenic abscesses) [45,46].

In atypical cases in which the abscess capsule shows T2 hyperintensity and T1 hypo/isointensity, differential diagnosis with other lesions is very difficult by using morphological MRI, and it can be improved with advanced MRI techniques.

Necrotic brain tumors

Necrotic brain tumors can be high-grade gliomas (HGGs) and metastases. They usually have a T2 hypointense peripheral

rim but it is often not complete as in the pyogenic abscesses. After gadolinium injection, HGGs show non-homogeneous enhancement with some nodular areas of enhancement protruding in the central cavity (Fig. 8). Metastases, on the other hand, can have a regular rim of enhancement similarly to pyogenic abscesses (Fig. 9). As a rule, necrotic brain tumors are hypointense, in the central area, in DWI (with high ADC values) (Figs. 8 and 9). However, DWI hyperintensity and low ADC have been described in necrotic metastases from lung, breast, colorectal and testicular cancer, and in bladder transitional cell carcinoma; nevertheless, this seems to be a very rare finding [44,47–49].

Furthermore, an intratumoral hemorrhage can increase the DWI signal [50] but the differential diagnosis is easy on the morphological images in which blood has typical signal changes over time.

On ^1H -MRS, presence of amino acids, acetate and succinate is typical for cerebral abscess [8,33].

Moreover, HGGs and metastases typically show an increase of neoangiogenesis with higher values of rCBV than abscesses in the periphery of the mass (Figs. 8 and 9) [35–39,51,52].

Finally, using susceptibility weighted imaging (SWI) (a new MR sequence enhancing the paramagnetic property of brain tissue), Toh et al. described a "double rim" hypointensity sign present in most of the abscesses and in none of the necrotic gliomas [70]; this can be another useful sign in the differential diagnosis between abscesses and necrotic tumors.

Fungal abscesses

Fungal abscesses are quite rare [54] and they can show, like pyogenic abscesses, a "ring-like" enhancement and a central hyperintense area on DWI with low ADC values [53,55] (Fig. 10).

Some fungal infections (i.e. aspergillosis) can invade brain vessels leading to hemorrhagic strokes that are extremely rare in pyogenic infections [57]. The finding of hemorrhagic strokes in basal ganglia and/or in thalamus in a patient with a primary aspergillosis (lungs, paranasal sinuses, etc.) is strongly suggestive of cerebral aspergillosis.

Sometimes the central cavity of fungal abscesses has heterogeneous signal on T2-w images because of the presence of hypointense areas with restricted diffusion and without contrast enhancement, representing zones of active fungal proliferations [8].

At ^1H -MRS, fungal abscesses show peaks of lipids, lactate and amino acids similarly to pyogenic abscesses.

Tuberculoma and tubercular abscesses

Tuberculoma typically shows a hypointense T2 peripheral rim and a "ring-like" contrast enhancement after injection of gadolinium [58]. The centre of the lesion shows iso/hypointensity in T1-w images and variable T2 signal related to the presence of caseous or liquefactive necrosis [58,59].

Three different kind of tuberculomas have been described according to T2 and ADC features [60]:

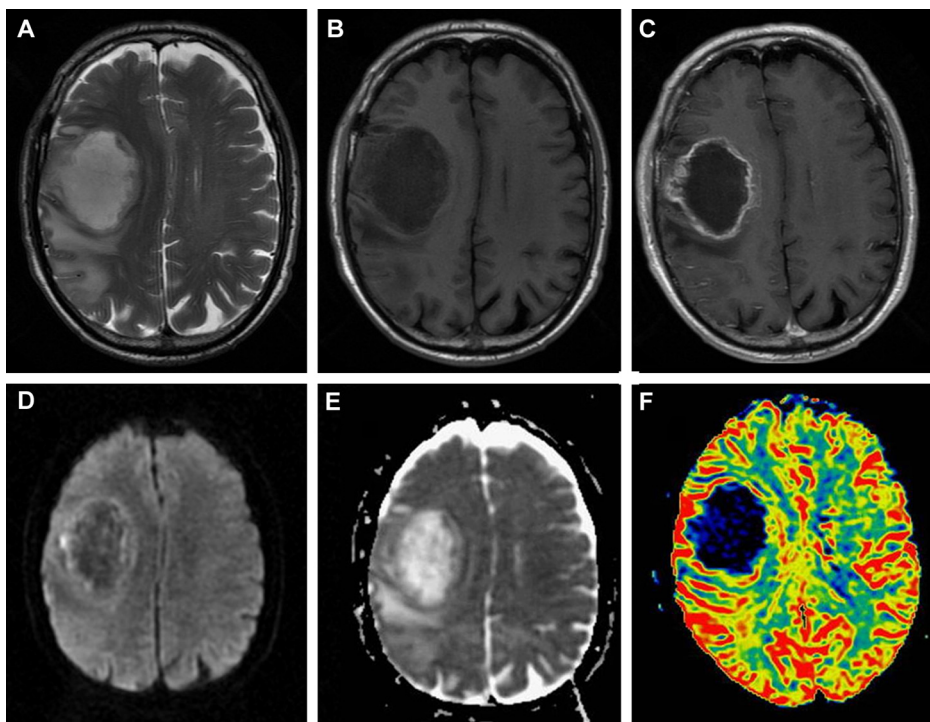


Figure 8 A–F: glioblastomas: T2-weighted (A), T1-weighted (B) and gadolinium-enhanced T1-weighted (Gd-MR) (A) images, DWI ($b=1000$) (D), ADC map (E) and map of CBV (F). The images show a lesion with hyperintense in T2 (A) and isointense in T1 (B) capsule. At Gd-MR image (C), the lesion shows a rim-enhancing mass with irregular margins surrounding vasogenic edema. The central component of the lesion shows iso-hyperintensity in DWI (D) and high signal intensity in the ADC map (E), findings that are consistent with increased diffusion. At PWI, the CBV map (F) shows increased perfusion in the Gd-enhancing rim of the lesion.

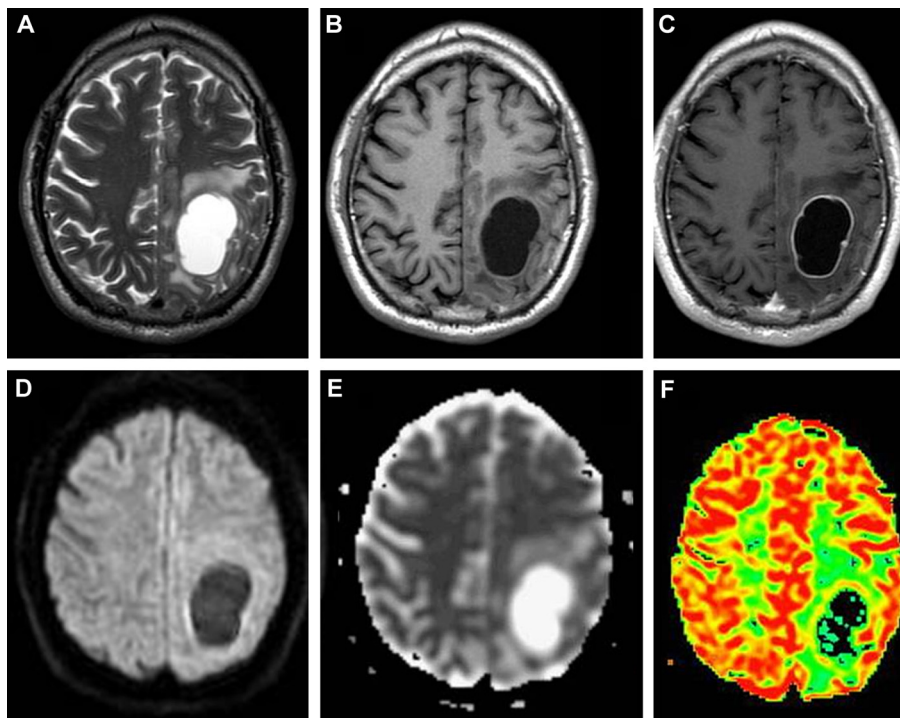


Figure 9 A–F: metastasis from colon cancer: T2-weighted (A), T1-weighted (B) and gadolinium-enhanced T1-weighted (Gd-MR) (A) images, DWI ($b=1000$) (D), ADC map (E) and map of CBV (F). The images show a lesion with a T2-hyperintense (A) and T1-isointense (B) capsule. At Gd-MR image (C), the metastatic lesion shows a rim-enhancing mass with regular margins. The central component of the lesion shows hypointensity at DWI (D) and high signal intensity in the ADC map (E), findings that are consistent with increased diffusion. At PWI, the CBV map (F) shows increased perfusion in the Gd-enhancing rim of the lesion.

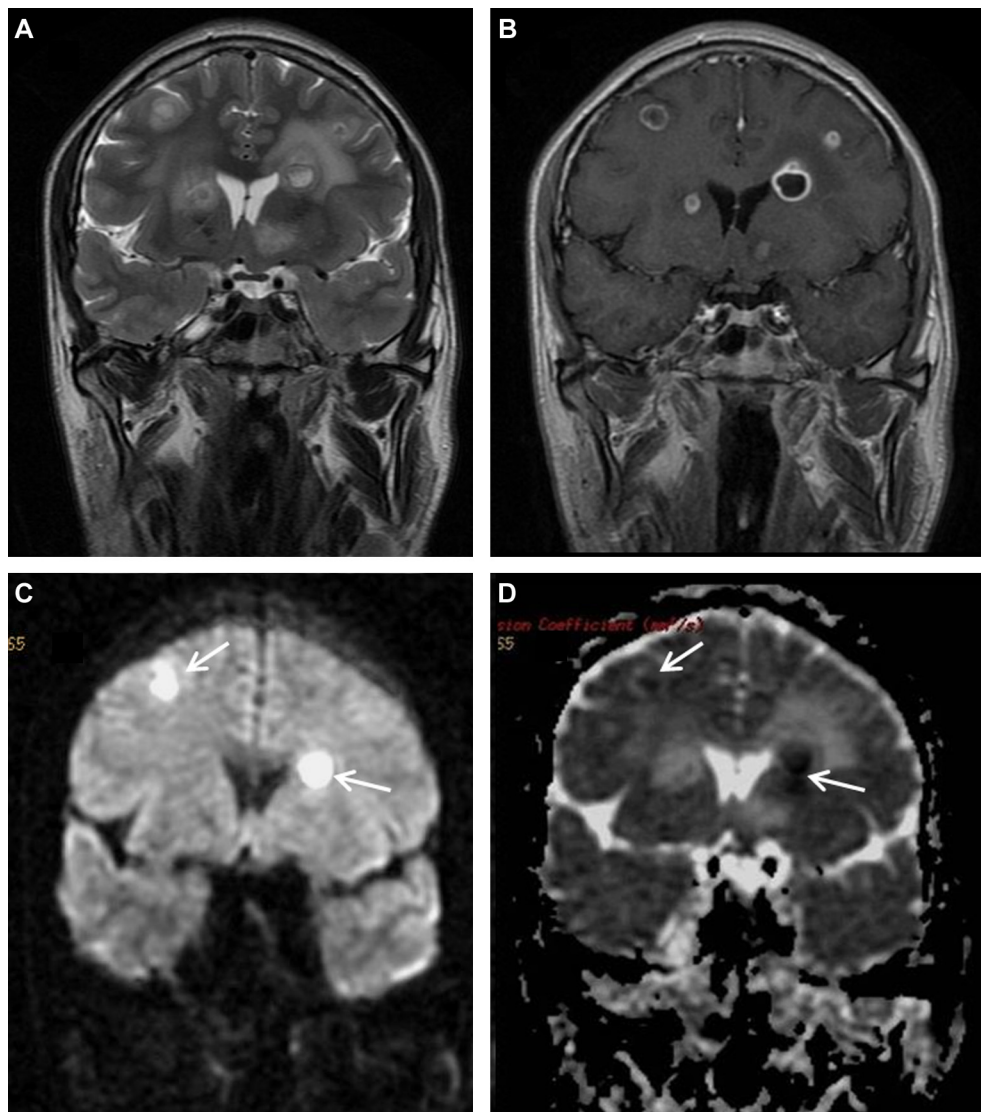


Figure 10 A–D: multiple fungal abscesses in immunocompromised patient: T2-weighted (A), Gadolinium-enhanced T1-weighted (Gd-RM) (B) images, DWI ($b = 1000$) (C), ADC map (D). At Gd-MRI image (B), the lesions show rim-enhancing masses. The central component of the lesions (arrows) shows high signal intensity in DWI image (C), and hypointense signal in ADC map (D), findings that are consistent with restricted diffusion.

- type I: hypointense core in T2 (caseous necrosis) with high ADC values ($1.24 \pm 0.32 \times 10^{-3} \text{ mm}^2/\text{s}$);
- type II: slightly hyperintense core in T2, with intermediate ADC values ($0.80 \pm 0.08 \times 10^{-3} \text{ mm}^2/\text{s}$);
- type III: strongly hyperintense core in T2, with lower ADC values ($0.74 \pm 0.13 \times 10^{-3} \text{ mm}^2/\text{s}$), consistent with liquefactive necrosis.

Furthermore, tuberculous meningitis is often associated with tuberculous meningitis that typically involves basal meninges [59] (Fig. 11).

Tuberculous abscess is rare, more commonly in immunocompromised patients [60,61]. It appears similar to pyogenic abscess at MRI, and can be single or multiple and often multiloculate with thin and regular borders [8]. The central area shows low ADC values as in pyogenic abscesses [8,58,60]. $^1\text{H}-\text{MRS}$ shows only peaks of lipids without any other peak [8];

this finding seems to be useful in the differential diagnosis among these two entities.

PWI can demonstrate high values of rCBV in the periphery of the mass, more similar to the values of HGGs than pyogenic abscesses [62].

Cerebral toxoplasmosis

Cerebral toxoplasmosis is typical of immunocompromised patients.

MRI demonstrates multiple lesions in different stages of evolution (Fig. 12), typically located in the subcortical and periventricular white matter, in the basal ganglia and thalamus (rarely in cerebellum) [63–65]. The presence of an eccentric area of contrast enhancement ("eccentric target sign") is a typical feature of cerebral toxoplasmosis (Fig. 12 C and F). The "concentric target sign" is a recently

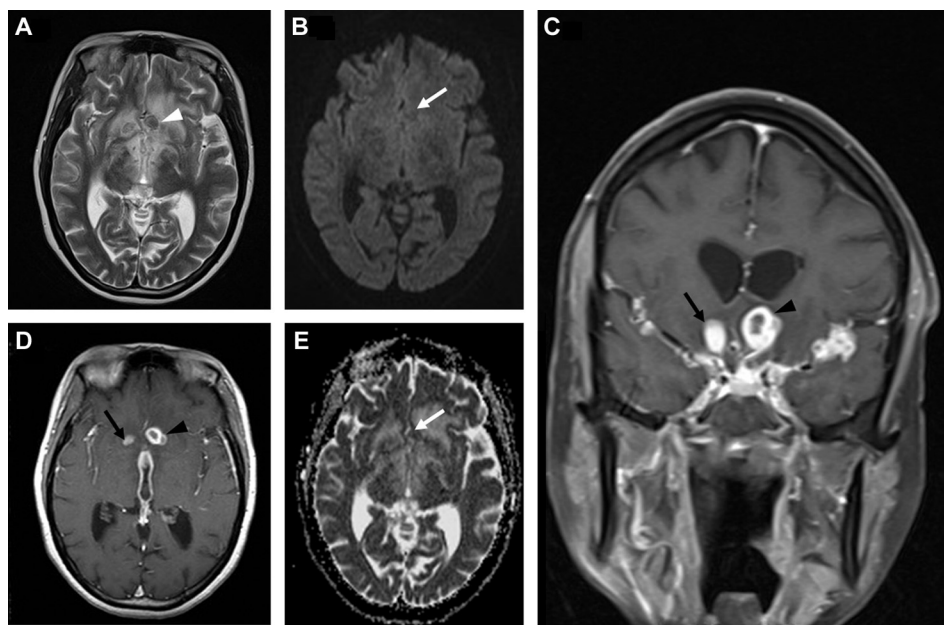


Figure 11 A–E: tuberculoma associated with tuberculum meningitis: T2-weighted (A), DWI ($b = 1000 \text{ s/mm}^2$) (B), gadolinium-enhanced T1-weighted coronal (Gd-MR) (C) and axial (D), ADC map (E) magnetic resonance images. The central part of the tuberculomas (group II) shows mildly hyperintensity in T2-weighted image (white arrowhead) (A), isointensity in DWI (B) and ADC map (white arrows) (E) with intermediate ADC value ($0.81 \times 10^{-3} \text{ mm}^2/\text{sec}$). At Gd-MRI images (C, D), the tuberculomas appears as rim-enhancing mass with thick margins. It is associated with tuberculous meningitis that typically affects the basal meninges, and ependymitis of the third ventricle; there are also tuberculous granuloma (black arrow) and other tuberculomas adjacent to the basal sylvian fissure.

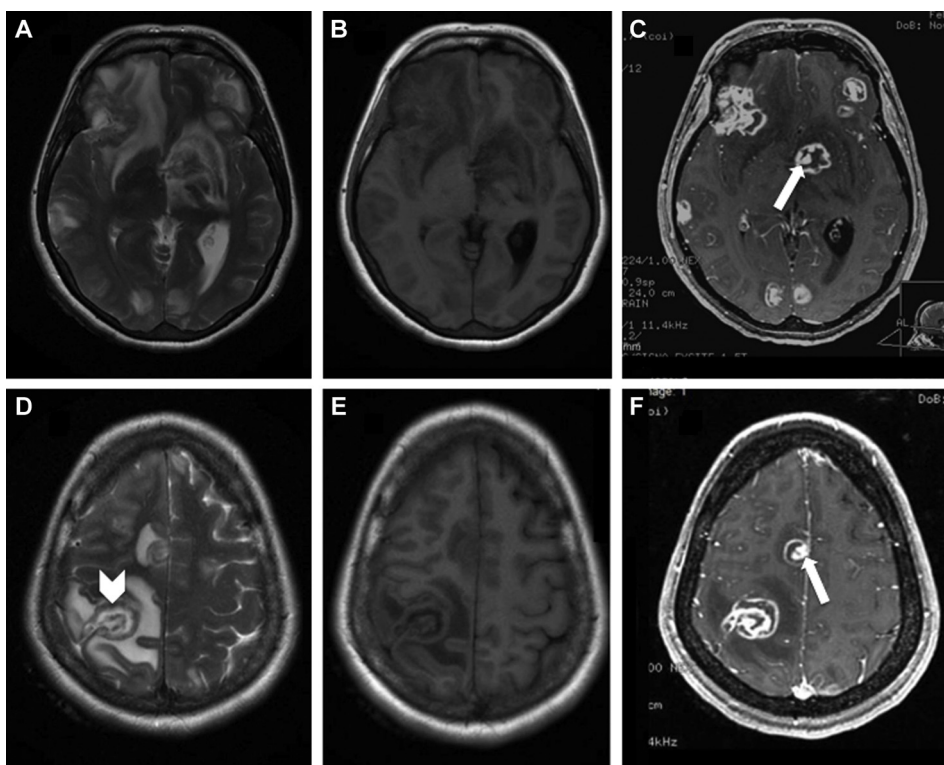


Figure 12 A–F: multiple *Toxoplasma gondii* abscesses: T2-weighted (A, D), T1-weighted (B, E) and gadolinium-enhanced T1-weighted resonance magnetic (Gg-MR) (C, F) images. Multiple supratentorial abscesses in various stages of development with "starry sky" appearance and enhancing asymmetric nodules ("eccentric target sign") (arrows) in Gg-MR images (C, F). Note also the concentric alternating zones of hypo- and hyperintensities in T2-weighted images: "concentric target sign" (D) (arrowheads).

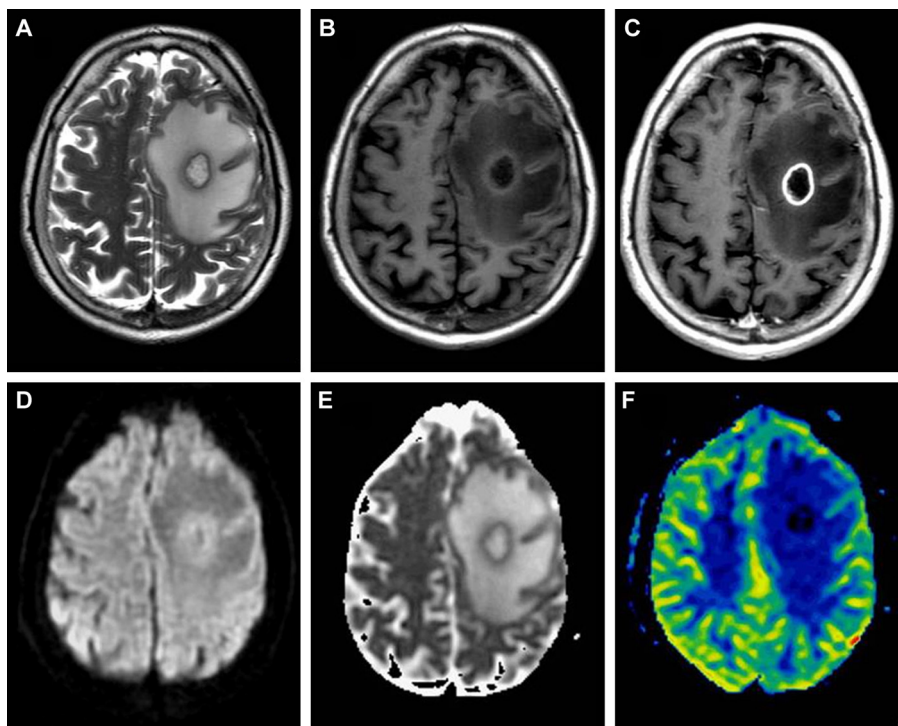


Figure 13 A–F: *Toxoplasma gondii* abscess in immunocompromised patient: T2-weighted (A), T1-weighted (B) and gadolinium-enhanced T1-weighted magnetic resonance (Gd-MR) (C) images, DWI ($b = 1000$) (D), ADC (E) and map of cerebral blood volume (CBV) perfusion weighted imaging (PWI) (F). The lesion shows ring enhancement with extensive perilesional vasogenic oedema. The centre of the lesion shows isointense signal in DWI (D), hyperintense signal in the ADC map (E) reflecting increased diffusion. At PWI, the CBV map (F) does not show evidence of increased perfusion in the capsule of the abscess.

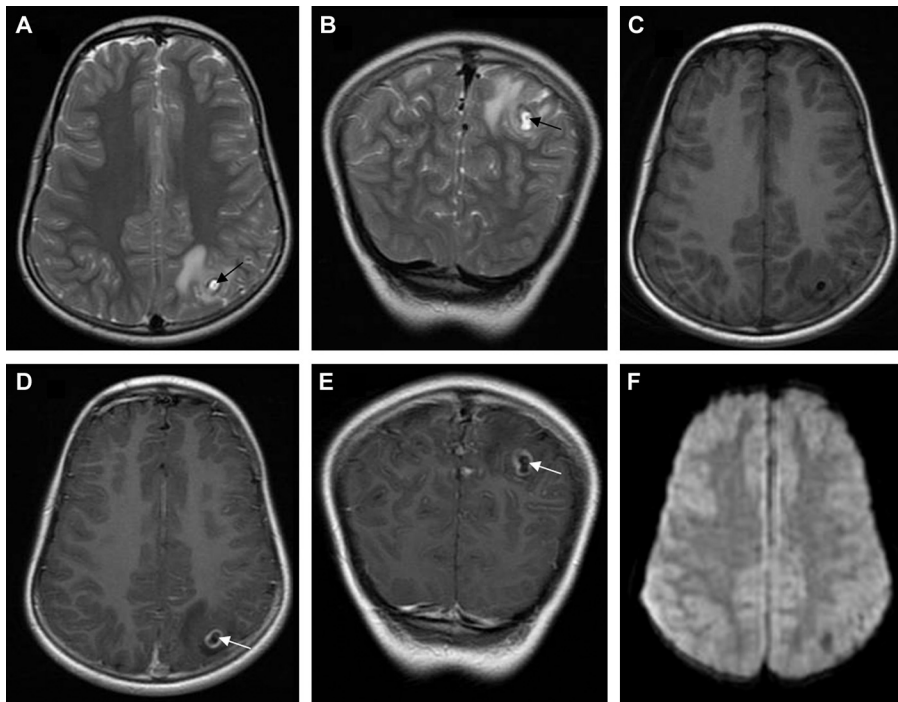


Figure 14 A–F: neurocystercosis in colloidal-vesicular stage: T2-weighted axial (A) and coronal (B), T1-weighted axial (C), gadolinium-enhanced T1-weighted axial (Gd-MR) (D) and coronal (E) MR images, DWI (F). At Gd-MR images (D, E) the lesion shows a rim-enhancing mass and in T2-weighted images the capsule is hypointense (A, B). The MR images show the scolex as a hypointense eccentric nodule in T2 (black arrows) and enhanced nodule in Gd-MR (white arrows). The central part of the lesion appears hypointense in DWI (E), finding that is consistent with increased diffusion.

described MRI sign on T2-weighted imaging which consists of concentric alternating zones of hypo- and hyperintensities (Fig. 12D). The "concentric target sign" seems to be more specific than the "eccentric target sign" in the diagnosis of cerebral toxoplasmosis especially in the context of AIDS [56].

DWI can be useful for differential diagnosis [36,58,67], since the centre of the toxoplasma abscess has a hypo/isointense signal in DWI with ADC values higher than in pyogenic abscesses (Fig. 13). On the contrary, PWI and ¹H-MRS seem to be not useful in distinguishing toxoplasmosis from a pyogenic abscess: PWI shows in both pyogenic abscesses and in cerebral toxoplasmosis a reduced perfusion in the capsule (Fig. 13) with a reported rCBV mean value of 0.84 ± 0.07 [66]; ¹H-MRS has low specificity because of the wide range of possible peaks [67,68].

Neurocysticercosis

MR features of neurocysticercosis change according to the stage of cyst evolution. Cysts in the colloidal-vesicular stage show hypointense core on T1-w and hyperintense on T2-w images, with a T2 hypointense pseudo-capsule and peripheral enhancement, with a surrounding oedema as in case of pyogenic abscesses. The scolex appears as an eccentric hypointense nodule on T2-w images that shows intense contrast enhancement (Fig. 14). In contrast to pyogenic abscess, the cyst in case of neurocysticercosis has high ADC values (Fig. 14) [69].

PWI shows a reduction of rCBV and thus, is not useful in differential diagnosis with pyogenic infection [77]. It is important to mention the intraventricular form of neurocysticercosis that has a rapidly progressive course and it is seen in more than 54% of patient with intracranial cysticercosis [69,71].

Conclusion

MRI is a useful tool for diagnosis, differential diagnosis, treatment planning and follow-up of pyogenic brain abscesses. Particularly the combined use of morphological and advanced techniques together, using the data from literature, is now critical in the diagnostic approach to abscess-like masses in the brain.

Disclosure of interest

Carmine F. Muccio, Ferdinando Caranci, Felice D'Arco, Alfonso Cerase, Luca De Lipsis, Gennaro Esposito, Enrico Tedeschi and Cosma Andreula declare that they have no conflicts of interest concerning this article.

References

- [1] Osenbach RK, Loftus CM. Diagnosis and management of brain abscess. *Neurosurg Clin North Am* 1992;3:403–20.
- [2] Carpenter J, Stapleton S, Holliman R. Retrospective analysis of 49 cases of brain abscess and review of the literature. *Eur J Clin Microbiol Infect Dis* 2007;26:1–11.
- [3] Hakan T, Ceran N, Erdem I, et al. Bacterial brain abscesses: an evaluation of 96 cases. *J Infect* 2006;52:359–66.
- [4] Kao PT, Tseng HK, Liu CP, et al. Brain abscess: clinical analysis of 53 cases. *J Microbiol Immunol Infect* 2003;36:129–36.
- [5] Seydoux C, Francioli P. Bacterial brain abscesses: factors influencing mortality and sequelae. *Clin Infect Dis* 1992;15:394–401.
- [6] Nowak DA, Rodick SO, Topka H. Pyogenic brain abscess following haematogenous seeding of a thalamic haemorrhage. *Neuroradiology* 2003;45:157–9.
- [7] Greenberg JO. *Neuroimaging*. 2nd edn Italia, Milano: McGraw-Hill; 2001.
- [8] Luthra G, Parihar A, Nath K, et al. Comparative evaluation of fungal, tubercular, and pyogenic brain abscesses with conventional and diffusion MR imaging and proton MR spectroscopy. *AJNR Am J Neuroradiol* 2007;28:1332–8.
- [9] Osborn A. *Diagnostic imaging: brain*. 1st edn Salt Lake City, Utah: Amirsys; 2004.
- [10] Parker Jr JC, Dyer MC. Neurologic infections due to bacteria, fungi and parasites. In: Doris RL, Robertson DM, editors. *Textbook of Neuropathology*. Baltimore: Williams & Wilkins; 1985. p. 632–70.
- [11] Erdogan E, Cansever T. Pyogenic brain abscess. *Neurosurg Focus* 2008;24(6):E2.
- [12] Schwartz KM, Erickson BJ, Lucchinetti C. Pattern of T2 hypointensity associated with ring-enhancing brain lesions can help to differentiate pathology. *Neuroradiology* 2006;48:143–9.
- [13] Haimes AB, Zimmerman RD, Morgello S, et al. MR imaging of brain abscesses. *AJR Am J Roentgenol* 1989;152:1073–85.
- [14] Falcone S, Post MJ. Encephalitis, cerebritis and brain abscess: pathophysiology and imaging findings. *Neuroimaging Clin N Am* 2000;10:333–53.
- [15] Cartes-Zulmelzu FW, Stavrou Ioannis, Castillo M, et al. Diffusion-weighted imaging in the assessment of brain abscesses therapy. *AJNR Am J Neuroradiol* 2004;25:1310–7.
- [16] Ebisu T, Tanaka C, Umeda M, et al. Discrimination of brain abscess from necrotic or cystic tumors by diffusion-weighted echo planar imaging. *Magn Reson Imaging* 1996;14:1113–6.
- [17] Kim YJ, Chang KH, Song IC, et al. Brain abscess and necrotic or cystic brain tumor: discrimination with signal intensity on diffusion-weighted MR imaging. *AJR Am J Roentgenol* 1998;171:1487–90.
- [18] Noguchi K, Watanabe N, Nagayoshi T, et al. Role of diffusion-weighted echo-planar MRI in distinguishing between brain abscess and tumor: a preliminary report. *Neuroradiology* 1999;41:171–4.
- [19] Desprechins B, Stadnik T, Koerts G, et al. Use of diffusion-weighted MR imaging in differential diagnosis between intracerebral necrotic tumors and cerebral abscesses. *AJNR Am J Neuroradiol* 1999;20:1252–7.
- [20] Mishra AM, Gupta RK, Saksena S, et al. Biological correlates of diffusivity in brain abscess. *Magn Reson Med* 2005;54:878–83.
- [21] Hartmann M, Jansen O, Heiland S, et al. Restricted diffusion within ring enhancement is not pathognomonic for brain abscess. *AJNR Am J Neuroradiol* 2001;22:1738–42.
- [22] Lee EJ, Ahn KJ, Ha YS, et al. Unusual findings in cerebral abscess: report of two cases. *Br J Radiol* 2006;79:e156–61.
- [23] Rana S, Albayram S, Lin DD, et al. Diffusion-weighted imaging and apparent diffusion coefficient maps in a case of intracerebral abscess with ventricular extension. *AJNR Am J Neuroradiol* 2002;23:109–12.
- [24] Duprez TP, Cosnard G, Hernalsteen D. Diffusion-weighted monitoring of conservative treated pyogenic brain abscesses: a marker for antibacterial treatment efficacy. *AJNR Am J Neuroradiol* 2005;26:1296–8.
- [25] Fanning NF, Laffan EE, Shroff MM. Serial diffusion-weighted MRI correlates with clinical course and treatment response

- in children with intracranial pus collection. *Pediatr Radiol* 2006;36:26–37.
- [26] Gupta RK, Vatsal DK, Husain N, et al. Differentiation of tuberculous from pyogenic brain abscesses with in vivo proton MR spectroscopy and magnetization transfer MR imaging. *AJNR Am J Neuroradiol* 2001;22:1503–9.
- [27] Grand S, Passaro G, Ziegler A, et al. Necrotic tumor versus brain abscess: importance of amino acids detected at ^1H MRS spectroscopy. Initial results. *Radiology* 1999;213:785–93.
- [28] Rémy C, Grand S, Laï ES, et al. ^1H MRS of human brain abscesses in vivo and in vitro. *Magn Reson Med* 1995;34:508–14.
- [29] Mendz GL, McCall MN, Kuchel PW. Identification of methyl resonances in the ^1H NMR spectrum of incubated blood cell lysate. *J Biol Chem* 1989;264:2100–7.
- [30] Vajro P, Sokal EM, Maddaluno S, et al. Brain abscess due to *Klebsiella pneumoniae* in a liver-transplanted child. *Transpl Infect Dis* 2009;11:341–5.
- [31] Pal D, Bhattacharyya A, Husain M, et al. In vivo proton MR spectroscopy evaluation of pyogenic brain abscesses: a report of 194 cases. *AJNR Am J Neuroradiol* 2010;31:360–6.
- [32] Lai PH, Li KT, Hsu SS, et al. Pyogenic brain abscess: findings from in vivo 1.5-T and 11.7-T in vitro proton MR spectroscopy. *AJNR Am J Neuroradiol* 2005;26:279–88.
- [33] Lai PH, Ho JT, Chen WL, et al. Brain abscess and necrotic brain tumor. Discrimination with proton MR spectroscopy and diffusion-weighted imaging. *AJNR Am J Neuroradiol* 2002;23:1369–77.
- [34] Kimura T, Sako K, Gotoh T, et al. In vivo single-voxel proton MR spectroscopy in brain lesion with ring-like enhancement. *NMR Biomed* 2001;14:339–49.
- [35] Erdogan C, Hakyemez B, Yildirim N, et al. Brain abscess and cystic brain tumor: discrimination with dynamic susceptibility contrast perfusion-weighted MRI. *J Comput Assist Tomogr* 2005;29:663–7.
- [36] Muccio CF, Esposito G, Bartolini A, et al. Cerebral abscesses and necrotic cerebral tumors: differential diagnosis by perfusion-weighted magnetic resonance imaging. *Radiol Med* 2008;113:747–57.
- [37] Holmes TM, Petrella JR, Provenzale JM. Distinction between cerebral abscesses and high-grade neoplasms by dynamic susceptibility contrast perfusion MRI. *AJR Am J Roentgenol* 2004;183:1247–52.
- [38] Chan JH, Tsui EY, Chau LF, et al. Discrimination of an infected brain tumor from a cerebral abscess by combined MR perfusion and diffusion imaging. *Comput Med Imaging Graph* 2002;26:19–23.
- [39] Haris M, Gupta RK, Singh A, et al. Differentiation of infective from neoplastic brain lesions by dynamic contrast-enhanced MRI. *Neuroradiology* 2008;50:531–40.
- [40] Britt RH, Enzmann DR, Yeager AS. Neuropathological and computerized tomographic findings in experimental brain abscess. *J Neurosurg* 1981;55:590–603.
- [41] Jenkins JR, Gupta R, Chang KH, Carballo-Rodriguez J. MR imaging of central nervous tuberculosis. *Radiol Clin North Am* 1995;33:771–86.
- [42] Gupta RK, Roy R. MR imaging and spectroscopy of intracranial tuberculomas. *Curr Sci* 1999;76:783–8.
- [43] Gupta RK, Roy R, Poptani H, et al. Finger printing of *Mycobacterium tuberculosis* in intracranial tuberculomas using in vivo, ex vivo and in vitro proton spectroscopy. *Magn Reson Med* 1996;36:829–33.
- [44] Holtas S, Geijer B, Stromblad LG, et al. A ring-enhancing metastasis with central high signal on diffusion-weighted imaging and low apparent diffusion coefficients. *Neuroradiology* 2000;42:824–7.
- [45] Janardhan V, Suri S, Bakshi R. Multiple sclerosis: hyperintense lesion in the brain on non-enhanced as areas of T1 shortening. *Radiology* 2007;244:823–31.
- [46] Osbron AG, Preece MT. Intracranial cyst: radiologic-pathologic correlation and imaging approach. *Radiology* 2006;239:650–64.
- [47] Park SH, Chang KH, Song IC, et al. Diffusion-weighted MRI in cystic or necrotic intracranial lesions. *Neuroradiology* 2000;42:716–21.
- [48] Tung GA, Evangelista P, Rogg JM, et al. Diffusion-weighted MR imaging of rim-enhancing brain masses: is markedly decreased water diffusion specific for brain abscess? *AJR Am J Roentgenol* 2001;177:709–12.
- [49] Duygulu G, Ovali GY, Calli C, et al. Intracerebral metastasis showing restricted diffusion: correlation with histopathologic findings. *Eur J Radiol* 2010;74:117–20.
- [50] Mori H, Abe O, Aoki S, et al. Hemorrhagic brain metastases with high signal intensity on diffusion-weighted MR images. *Acta Radiol* 2002;43:563–6.
- [51] Chiang IC, Hsieh TJ, Chiu ML, et al. Distinction between pyogenic brain abscess and necrotic brain tumor using 3-tesla MR spectroscopy, diffusion and perfusion imaging. *Br J Radiol* 2009;82:813–20.
- [52] Fertikh D, Krejza J, Cunqueiro A, et al. Discrimination of capsular stage brain abscesses from necrotic or cystic neoplasm using diffusion-weighted magnetic resonance imaging. *J Neurosurg* 2007;106:76–81.
- [53] Castro S, Bernardes I. Coccidioidal cerebral abscess with peripheral restricted diffusion. *J Neuroradiol* 2009;36(3):162–4.
- [54] Kastrup O, Wanke I, Maschke M. Neuroimaging of infection. *NeuroRX* 2005;2:324–32.
- [55] Gaviani P, Schwartz RB, Hedley-Whyte T, et al. Diffusion-weighted imaging of fungal cerebral infection. *AJNR Am J Neuroradiol* 2005;26:1115–21.
- [56] Mahadevan A, Ramalingaiah AH, Parthasarathy S, et al. Neuropathological correlate of the “concentric target sign” in MRI of HIV-associated cerebral toxoplasmosis. *J Magn Reson Imaging* 2013;38(2):488–95.
- [57] Miaux Y, Ribaud P, Williams M, et al. MR of cerebral aspergillosis in patient who have had bone marrow transplantation. *AJNR Am J Neuroradiol* 1995;16:555–62.
- [58] Batra A, Tripathi RP. Diffusion-weighted magnetic resonance imaging and magnetic resonance spectroscopy in the evaluation of focal cerebral tubercular lesions. *Acta Radiol* 2004;45:679–88.
- [59] Bernaerts A, Vanhoenacker FM, Parizel PM, et al. Tuberculosis of the central nervous system: overview of neuroradiological findings. *Neuroradiology* 2003;13:1876–90.
- [60] Gupta RK, Prakash M, Mishra AM, et al. Role of diffusion weighted imaging in differentiation of intracranial tuberculoma and tuberculous abscess from cysticercus granulomas—a report of more than 100 lesions. *Eur J Radiol* 2005.
- [61] Barnes PF, Bloch AB, Davidson PT, et al. Tuberculosis in patients with human immunodeficiency virus infection. *N Engl J Med* 1991;324:1644–50.
- [62] Batra A, Tripathi RP. Perfusion magnetic resonance imaging in intracerebral parenchymal tuberculosis: preliminary findings. *J Comput Assist Tomogr* 2003;27:882–8.
- [63] Navia BA, Petit CK, Gold JK, et al. Cerebral toxoplasmosis complicating the acquired immune deficiency syndrome: clinical and neuropathological findings in 27 patients. *Ann Neurol* 1986;19(3):224–38.
- [64] Ramsey RG, Geremia GK. CNS complications of AIDS: CT and MR findings. *AJR Am J Roentgenol* 1988;15:449–554.
- [65] Chong-Han C, Cortez SC, Tung GA. Diffusion-weighted MRI of cerebral toxoplasma abscess. *AJR Am J Roentgenol* 2003;181:1711–4.
- [66] Barcelo C, Catalaa I, Loubes-Lacroix F. Interest of MR perfusion and MR spectroscopy for the diagnostic of atypical cerebral toxoplasmosis. *J Neuroradiol* 2010;37(1):68–71.

- [67] Chinn RJ, Wilkinson ID, Hall-Craggs MA, et al. Toxoplasmosis and primary central nervous system lymphoma in HIV infection: diagnosis with MR spectroscopy. *Radiology* 1995;197:649–59.
- [68] Gupta RK. Magnetic resonance spectroscopy in intracranial infection. In: Gillard JH, Waldaman AD, Barker PB, editors. *Clinical MR neuroimaging*. New York: Cambridge University Press; 2010. p. 426–51.
- [69] Sinha S, Sharma BS. Intraventricular neurocysticercosis: a review of current status and management issues. *Br J Neurosurg* 2012;26(3):305–9.
- [70] Toh CH, Wei KC, Chang CH, et al. Differentiation of byogenic brain abscesses from necrotic glioblastoma with use of susceptibility-weighted imaging. *AJNR* 2012;33(8):1534–8.
- [71] Vandesteene L, Drier A, Galanaud D, Clarençon F, et al. Imaging findings of intraventricular and ependymal lesions. *J Neuroradiol* 2013;40(4):229–44.
- [72] Tokgoz S, Paksoy Y, Tokgoz H, Demir I, Mutler M. Perfusion-weighted cranial MR imaging findings in a patient with hemophagocytic lymphohistiocytosis. *J Neuroradiol* 2013;40(4):307–10.
- [73] Dashti SR, Baharvahdat H, Sauvageau E, et al. Brain abscess formation at the site of intracerebral hemorrhage secondary to central nervous system vasculitis. *Neurosurg Focus* 2008;24(6):E12.
- [74] Enzmann DR, Britt RH, Placone R. Staging of human brain abscess by computed tomography. *Radiology* 1983;146:703–8.
- [75] Domingo Z. Clostridial brain abscesses. *Br J Neurosurg* 1994;8:691–4.
- [76] Liliang PC, Lin YC, Su TM, et al. *Klebsiella* brain abscess in adults. *Infection* 2001;29:81–6.
- [77] do Amaral LL, Ferreira RM, da Rocha AJ, et al. Neurocysticercosis: evaluation with advanced magnetic resonance techniques and atypical forms. *Top Magn Reson Imaging* 2005;16:127–44.